

# Linear-Mapping based Variational Ensemble Kalman Filter

Linjie Wen, Jinglai Li

## Abstract

We propose a linear-mapping based variational Ensemble Kalman filter for problems with generic observation models. Specifically, the proposed method is formulated as to construct a linear mapping from the prior ensemble to the posterior one, and the linear mapping is computed by minimizing the Kullback-Leibler divergence between the transformed distribution by the linear mapping and the actual posterior. With numerical examples we demonstrate that the method has competitive performance against existing methods.

## Index Terms

ensemble Kalman filter, Kullback-Leibler divergence, linear mapping, observation model

## I. INTRODUCTION

The ensemble Kalman filter (EKF) [1] is one of the most popular tools for sequential Bayesian filtering problems, thanks to its computational efficiency and flexibility. Simply put, at each time step EKF approximates the prior, the likelihood and the posterior by Gaussian distributions. Such a Gaussian approximation allows a linear update that maps the prior ensemble to the posterior one. This linear update is the key that enables EKF to handle large-scale problems with a relatively small number of ensemble particles. In the conventional EKF, it is required that the observation model is Gaussian-linear, which means that the observation operator is linear and the noise is additive Gaussian. However, in many real-world applications, neither of these two requirements is satisfied.

To the end, it is of practical importance to develop EKF extensions that can deal with generic observation models, while retaining the computational advantage of EKF. A notable example of such methods is the nonlinear ensemble adjustment filter (NLEAF) [2], which involves a correction scheme: the posterior moments are calculated with importance sampling and the ensembles are then corrected accordingly. Other methods that be applied to such problems include [3]–[5] (some of them may need certain modifications), just to name a few. In this work we focus on the EKF type of methods that can use a small number of ensembles in high dimensional problems, and full Monte Carlo methods such as the particle filters (PF) [6] are not in our scope. The main purpose of this work is to provide an alternative framework to implement EKF for arbitrary observation models. Specifically, the proposed method formulates the EKF update as to construct a linear mapping/transform from the prior to the posterior and the linear mapping is computed by minimizing the Kullback-Leibler divergence (KLD) between the transformed distribution and the posterior. We note here that a similar formulation has been used in the variational Kalman filter [7]. It can be seen that this linear mapping based EKF (LMEKF) reduces to the standard EKF when the observation model is Gaussian-linear, and as such it is a natural generalization of the standard EKF to generic observation models. Also, by design the obtained linear mapping is *optimal* under the minimal KLD principle. With numerical examples we demonstrate that the method has competitive performance against existing methods.

L. Wen is with the School of Mathematical Science, Shanghai Jiao Tong University, Shanghai 200240, China.

J. Li is with the School of Mathematics, University of Birmingham, Birmingham B15 2TT, UK. e-mail: (j.li.10@bham.ac.uk).

Manuscript received \*\*\*.

## II. PROBLEM FORMULATION

### A. Hidden Markov Model

In this work we consider a generic hidden Markov model (HMM) formulation. Specifically let  $\{x_t\}$  and  $\{y_t\}$  for  $t > 0$  be two discrete-time stochastic processes, and the HMM of the pair  $\{x_t, y_t\}$  is in the following form,

$$x_t \sim f_t(\cdot|x_{t-1}), \quad (1a)$$

$$y_t \sim g_t(\cdot|x_t), \quad t = 1, \dots, T \quad (1b)$$

where  $T$  is a positive integer,  $f_t(\cdot|x_{t-1})$  and  $g_t(\cdot|x_t)$  are known conditional distributions, and  $x_t$  and  $y_t$  are respectively the hidden and the observed states. This framework represents many practical problems of interest, where one makes observations of  $\{y_t\}_{t=1}^T$  and estimates the hidden states  $\{x_t\}_{t=1}^T$  therefrom.

### B. Recursive Bayesian Filtering

Recursive Bayesian filtering [8] is a popular framework to estimate the hidden states in a HMM, and it aims to compute the condition distribution  $\pi(x_t|y_{1:t})$  for  $t = 1, \dots, T$  recursively. Throughout the paper, we use  $\pi$  as a generic notation of a probability distribution whose actual meaning is specified by its arguments. Next we discuss how the recursive Bayesian filtering proceeds. First applying the Bayes' formula, we obtain

$$\pi(x_t|y_{1:t}) = \frac{\pi(y_t|x_t, y_{1:t-1})\pi(x_t|y_{1:t-1})}{\pi(y_t|y_{1:t-1})}, \quad (2)$$

where  $\pi(y_t|y_{1:t-1})$  is the normalization constant that often does not need to be evaluated in practice. From Eq. (1) we know that  $y_t$  is independent of  $y_{t-1}$  conditionally on  $x_t$ , and thus Eq. (2) becomes

$$\pi(x_t|y_{1:t}) = \frac{g_t(y_t|x_t)\pi(x_t|y_{1:t-1})}{\pi(y_t|y_{1:t-1})}. \quad (3)$$

The condition distribution  $\pi(x_t|y_{1:t-1})$  can be expressed as

$$\pi(x_t|y_{1:t}) = \int \pi(x_t|x_{t-1}, y_{1:t-1})\pi(x_{t-1}|y_{1:t-1})dx_{t-1}, \quad (4)$$

and again thanks to the property of the HMM in Eq. (1), we have,

$$\pi(x_t|y_{1:t-1}) = \int f_t(x_t|x_{t-1})\pi(x_{t-1}|y_{1:t-1})dx_{t-1}, \quad (5)$$

where  $\pi(x_{t-1}|y_{1:t-1})$  is the posterior distribution at the previous step  $t - 1$ . As a result the recursive Bayesian filtering performs the following two steps in each iteration:

- Prediction step: the prior density  $\pi(x_t|y_{1:t-1})$  is determined via Eq. (5),
- Update step: the posterior density  $\pi(x_t|y_{1:t})$  is computed via Eq. (3).

The recursive Bayesian filtering provides a generic framework for sequentially computing the conditional distribution  $\pi(x_t|y_{1:t})$  as the iteration proceeds. In practice, the analytical expressions for the posterior  $\pi(x_t|y_{1:t})$  or the prior  $\pi(x_t|y_{1:t-1})$  usually can not be obtained, and have to be represented numerically, for example, by an ensemble of particles.

## III. LINEAR MAPPING BASED ENSEMBLE KALMAN FILTER

We describe the linear mapping based EKF in this section.

### A. Linear mapping based Bayesian update

We first consider the update step: namely suppose that the prior distribution  $\pi(x_t|y_{1:t-1})$  is obtained, and we want to compute the posterior  $\pi(x_t|y_{1:t})$ . We start with a brief introduction to the transport map based methods for computing the posterior distribution [9], where the main idea is to construct a mapping which pushes the prior distribution into the posterior. Namely suppose  $\tilde{x}_t$  follows the prior distribution  $\pi(\cdot|y_{1:t-1})$ , and one aims to construct a bijective mapping  $T : R^d \rightarrow R^d$ , such that  $x_t = T(\tilde{x}_t)$  follows the posterior distribution  $\pi(\cdot|y_{1:t})$ . In reality, it is often impossible to exactly push the prior into the posterior  $\pi(\cdot|y_{1:t})$ , and in this case an approximate approach can be used. That is, let  $\pi_T(\cdot)$  be the distribution of  $x_t = T(\tilde{x}_t)$  and we seek a mapping  $T \in \mathcal{H}$  where  $\mathcal{H}$  is a given function space, so that  $\pi_T(\cdot)$  is “closest” to the actual posterior  $\pi(\cdot|y_{1:t})$  in terms of certain measure of distance between two distributions. In practice, the KLD, which (for any two distributions  $\pi_1$  and  $\pi_2$ ) is defined as,

$$\mathcal{D}_{\text{KL}}(\pi_1, \pi_2) = \int \log \left[ \frac{\pi_1(x)}{\pi_2(x)} \right] \pi_1(x) dx \quad (6)$$

is often used for such a distance measure. That is, we find a mapping  $T$  by solving the following minimization problem,

$$\min_{T \in \mathcal{H}} \mathcal{D}_{\text{KL}}(\pi_T, \pi(x_t|y_{1:t})), \quad (7)$$

which can be regarded as a variational Bayes formulation.

To actually find the linear mapping, we need to address two key issues. The first is that, in practice, the prior distribution  $\pi(\tilde{x}_t|y_{1:t-1})$  is usually not analytically available, and in particular they are represented by an ensemble of particles. As is in the standard EKF, we assume that the prior distribution is reasonably close to Gaussian. As a result we can estimate a Gaussian approximation of the prior distribution  $\pi(\tilde{x}_t|y_{1:t-1})$  from the particle ensemble. Namely, given an ensemble  $\{\tilde{x}_t^m\}_{m=1}^M$  drawn from the prior distribution  $\hat{\pi}(\tilde{x}_t|y_{1:t-1})$ , we construct an approximate prior  $\hat{\pi}(\cdot|y_{1:t-1}) = N(\tilde{\mu}_t, \tilde{\Sigma}_t)$ , with

$$\tilde{\mu}_t = \frac{1}{M} \sum_{m=1}^M \tilde{x}_t^m, \quad (8a)$$

$$\tilde{\Sigma}_t = \frac{1}{M-1} \sum_{m=1}^M (\tilde{x}_t^m - \tilde{\mu}_t)(\tilde{x}_t^m - \tilde{\mu}_t)^T. \quad (8b)$$

As a result, Eq. (7) is modified to minimizing  $\mathcal{D}_{\text{KL}}(\pi_T, \hat{\pi}(x_t|y_{1:t}))$  where  $\hat{\pi}(x_t|y_{1:t})$  is the approximate posterior

$$\hat{\pi}(\cdot|y_{1:t}) \propto \hat{\pi}(\cdot|y_{1:t-1})g_t(y_t|x_t). \quad (9)$$

The second important issue is to specify a suitable function space  $\mathcal{H}$ , and we choose  $T$  to be a linear mapping. More precisely we let  $\mathcal{H}$  to be the space of linear and bijective functions, and the reason for such a choice is two-fold. First, from the computational perspective, since filtering often needs to be done sequentially and in realtime, the computational efficiency of a filtering algorithm is essential. To this end, solving the optimization problem Eq. (7) for a general function space can pose a serious computational challenge, while the use of linear mappings may considerably simplify the computation for solving Eq. (7). More importantly, a key assumption of the proposed method is that both the prior and posterior ensembles should not deviate strongly from Gaussian. To this end, a natural requirement for the chosen function space  $\mathcal{H}$  is that, for any  $T \in \mathcal{H}$ , if  $\pi(\tilde{x}_t|y_{1:t-1})$  is close to Gaussian, so should be  $\pi_T(x_t)$  with  $x_t = T(\tilde{x}_t)$ . Obviously an arbitrarily function space does not satisfy such a requirement. However, for linear mappings, we have the following proposition:

**Proposition 1.** *For a given positive constant number  $\epsilon$ , if there is a  $d$ -dimensional normal distribution  $\tilde{p}_G$  such that  $\mathcal{D}_{\text{KL}}(\tilde{p}_G(\tilde{x}_t), \pi(\tilde{x}_t|y_{1:t-1})) < \epsilon$ , and if  $T$  is a linear and bijective mapping, there must exist a  $d$ -dimensional normal distribution  $p_G$  satisfying  $\mathcal{D}_{\text{KL}}(p_G(x_t), \pi_T(x_t)) < \epsilon$ .*

This proposition is a direct consequence of the fact that KLD is invariant under linear transformations, and loosely the proposition states that, for a linear mapping  $T$ , if the prior  $\pi(\tilde{x}_t|y_{1:t-1})$  is close to a Gaussian distribution, so is  $\pi_T(x_t)$ , which ensures that the update step will not increase the “non-Gaussianity” of the particles.

---

**Algorithm 1** The Linear-mapping based ensemble Kalman filter (LMEKF)

---

- Prediction:
  - Let  $\tilde{x}_t^m \sim f_t(\cdot|x_{t-1}^m)$ ,  $m = 1, 2, \dots, M$ ;
  - Let  $\hat{\pi}(\cdot|y_{1:t-1}) = N(\tilde{\mu}_t, \tilde{\Sigma}_t)$  where  $\tilde{\mu}_t$  and  $\tilde{\Sigma}_t$  are computed using Eq. (8);
- Update:
  - Let  $\hat{\pi}(x_t|y_{1:t}) \propto \hat{\pi}(x_t|y_{1:t-1})g_t(y_t|x_t)$ ;
  - Solve the minimization problem:

$$T_t = \arg \min_{T \in \mathcal{L}} \mathcal{D}_{\text{KL}}(\pi_T, \hat{\pi}(x_t|y_{1:t})). \quad (10)$$

- Let  $x_t^m = T_t \tilde{x}_t^m$  for  $m = 1, \dots, M$ .
- 

### B. Ensemble Kalman Filter

In this section, we show that the standard EKF can be derived as a special case of LMEKF. We consider the situation where the observation model takes the form of

$$g_t(y_t|x_t) = N(H_t x_t, R_t).$$

Recall that it has been assumed in LMEKF that the prior is approximated as  $\hat{\pi}(\cdot|y_{1:t-1}) = N(\tilde{\mu}_t, \tilde{\Sigma}_t)$ , and it follows that the approximate posterior is also Gaussian:  $\hat{\pi}(\cdot|y_{1:t}) = N(\mu_t, \Sigma_t)$ . The mean  $\mu_t$  and the covariance  $\Sigma_t$  can be obtained analytically:

$$\mu_t = (I - K_t H_t) \tilde{\mu}_t + K_t y_t, \quad \Sigma_t = (I - K_t H_t) \tilde{\Sigma}_t \quad (11)$$

where  $I$  is the identity matrix and Kalman Gain matrix  $K_t$  is

$$K_t = \tilde{\Sigma}_t H_t^T (H_t \tilde{\Sigma}_t H_t^T + R_t)^{-1}. \quad (12)$$

In this case, the optimization problem (7) can be solved exactly where the optimal mapping is

$$x_t = T(\tilde{x}_t) = (I - K_t H_t) \tilde{x}_t + K_t y_t, \quad (13)$$

and the resulting value of KLD is zero, which means that the optimal mapping pushes the prior exactly to the posterior. One sees immediately that the optimal mapping in Eq (13) coincides with the updating formula of EKF, and thus we have verified that EKF can be derived as a special case of LMEKF when the observation model is linear-Gaussian. Finally we note that a simple extension of EKF to the generic observation model is available where the Kalman gain matrix is obtained via a sample estimate of the covariance between the state vector and the observation vector [5]. This extended EKF method will be compared against the proposed LMEKF in the numerical experiments.

### C. Numerical algorithm for minimizing KLD

In the LMEKF framework presented in section III-A, the key step is to solve KLD minimization problem (7). In this section we describe in details how the optimization problem is solved numerically. Namely suppose at step  $t$ , we have a set of samples  $\{\tilde{x}_t^m\}_{m=1}^M$  drawn from the prior distribution  $\pi(\tilde{x}_t|y_{1:t-1})$ , we want to transform them into the ensemble  $\{x_t^m\}_{m=1}^M$  that follows the approximate posterior  $\pi(x_t|y_{1:t})$ . First we set up some notations, and for conciseness some of them are different from those used in the

previous sections: first we drop the subscript of  $\tilde{x}_t$  and  $x_t$ , and we then define  $p(\tilde{x}) = \pi(\tilde{x}|y_{1:t-1})$  (the actual prior),  $\hat{p}(\tilde{x}) = \tilde{\pi}(\tilde{x}|y_{1:t-1}) = N(\tilde{\mu}, \tilde{\Sigma})$  (the Gaussian approximate prior),  $l(x) = -\log \pi(y_t|x)$  (the negative log-likelihood) and  $q(x) = \hat{\pi}(x|y_{1:t})$  (the approximate posterior).

Recall that we want to minimize  $\mathcal{D}_{\text{KL}}(p_T(x), q(x))$  where  $p_T$  is the distribution of the transformed random variable  $x = T(\tilde{x})$ , and it is easy to show that

$$\mathcal{D}_{\text{KL}}(p_T(x), q(x)) = \mathcal{D}_{\text{KL}}(p(\tilde{x}), q_{T^{-1}}(\tilde{x})),$$

where  $q_{T^{-1}}$  is the distribution of the inversely transformed random variable  $\tilde{x} = T^{-1}(x)$  with  $x \sim q(x)$ . Moreover, since,

$$\begin{aligned} \mathcal{D}_{\text{KL}}(p(\tilde{x}), q_{T^{-1}}(\tilde{x})) \\ = \int \log[p(\tilde{x})]p(\tilde{x})d\tilde{x} - \int \log[q_{T^{-1}}(\tilde{x})]p(\tilde{x})d\tilde{x}, \end{aligned}$$

minimizing  $\mathcal{D}_{\text{KL}}(p_T(x), q(x))$  is equivalent to

$$\max_{T \in \mathcal{L}} \int \log[q_{T^{-1}}(\tilde{x})]p(\tilde{x})d\tilde{x}. \quad (14)$$

Since the function space  $\mathcal{L}$  represents linear and bijective mappings, we can write it as

and thus we just need determine the matrix  $A$  and the vector  $b$ . Moreover,  $q_{T^{-1}}(\tilde{x})$  can be written as,

$$q_{T^{-1}}(\tilde{x}) = q(A\tilde{x} + b)|A|, \quad (15)$$

and we now substitute Eq. (15) along with Eq. (9) in to Eq. (14), yielding,

$$\begin{aligned} \min_{A,b} F_q(A, b) &:= - \int \log[q(A\tilde{x} + b)]p(\tilde{x})d\tilde{x} - \log |A| \\ &= - \int \log[\tilde{p}(A\tilde{x} + b)]p(\tilde{x})d\tilde{x} \\ &\quad - \int l(A\tilde{x} + b)p(\tilde{x})d\tilde{x} - \log |A| \\ &= \frac{1}{2} \text{Tr}[(\tilde{\Sigma} + \tilde{\mu}\tilde{\mu}^T)A^T\tilde{\Sigma}^{-1}A] \\ &\quad + (b - \tilde{\mu})^T\tilde{\Sigma}^{-1}[A\tilde{\mu} + \frac{1}{2}(b - \tilde{\mu})] - \log |A| \\ &\quad - \mathbb{E}_{\tilde{x} \sim p}[l(A\tilde{x} + b)] + \frac{1}{2}(d \log(2\pi) + \log |\tilde{\Sigma}|). \quad (16) \end{aligned}$$

We then solve the optimization problem (16) with a gradient descent (GD) scheme:

$$\begin{aligned} A_{k+1} &= A_k - \epsilon_k \frac{\partial F_q}{\partial A}(A_k, b_k), \\ b_{k+1} &= b_k - \epsilon_k \frac{\partial F_q}{\partial b}(A_k, b_k), \end{aligned}$$

where  $\epsilon_k$  is the step size and the gradients can be derived as,

$$\begin{aligned} \frac{\partial F_q}{\partial A}(A, b) &= (\tilde{\Sigma} + \tilde{\mu}\tilde{\mu}^T)A^T\tilde{\Sigma}^{-1} + \tilde{\Sigma}^{-1}(b - \tilde{\mu})\tilde{\mu}^T \\ &\quad - A^{-1} - \mathbb{E}_{\tilde{x} \sim p}[\nabla_x l(A\tilde{x} + b)\tilde{x}^T], \quad (17a) \end{aligned}$$

$$\frac{\partial F_q}{\partial b}(A, b) = \tilde{\Sigma}^{-1}[A\tilde{\mu} + b - \tilde{\mu}] - \mathbb{E}_{\tilde{x} \sim p}[\nabla_x l(A\tilde{x} + b)]. \quad (17b)$$

Note that Eq. (17) involves the expectations  $E_{\tilde{x} \sim p}[\nabla_x l(A\tilde{x} + b)\tilde{x}^T]$  and  $E_{\tilde{x} \sim p}[\nabla_x l(A\tilde{x} + b)]$  which are not known exactly, and in practice they can be replaced by their Monte Carlo estimates:

$$E_{\tilde{x} \sim p}[\nabla_x l(A\tilde{x} + b)\tilde{x}^T] \approx \frac{1}{M} \sum \nabla_x l(A\tilde{x}^m + b)(\tilde{x}^m)^T,$$

$$E_{\tilde{x} \sim p}[\nabla_x l(A\tilde{x} + b)] \approx \frac{1}{M} \sum_{m=1}^M \nabla_x l(A\tilde{x}^m + b),$$

where  $\{\tilde{x}^m\}_{m=1}^M$  are the prior ensemble and  $\nabla_x l(x)$  is the derivative of  $l(x)$  taken with respect to  $x$ . The same Monte Carlo treatment also applies to the objective function  $F_q(A, b)$  itself when it needs to be evaluated.

The last important ingredient of the optimization algorithm is the stopping criteria. Due to the stochastic nature of the optimization problem, standard stopping criteria in the gradient descent method are not effective here. Therefore we adopt a commonly used criterion in search-based optimization: the iteration is terminated if the current best value is not sufficiently increased within a given number of steps. More precisely, let  $F_k^*$  and  $F_{k-\Delta k}^*$  be the current best value at iteration  $k$  and  $k - \Delta k$  respectively, and the iteration is terminated if  $F_k^* - F_{k-\Delta k}^* < \Delta_F$  for a prescribed threshold  $\Delta_F$ .

Finally it is important to mention that the EKF type of methods are often applied to problems where the ensemble size is smaller than the dimensionality of the states and in this case the localization techniques are usually used to address the undersampling issue. In the LMEKF method, all the localization techniques developed in EKF can be directly used, and in our numerical experiments we adopt the sliding-window localization used in [10].

#### IV. NUMERICAL EXAMPLES

##### A. Observation model

As is mentioned earlier, the goal of this work is to deal with generic observation models, and in our numerical experiments, we test the proposed method with an observation model that is quite flexible and also commonly used in reality [11]:

$$y_t = g(x_t, \beta_t) = M(x_t) + aM(x_t)^\theta \circ \beta_t, \quad (18)$$

where  $M(\cdot) : R^d \rightarrow Y$  is a mapping from the state space to the observation space  $Y$ ,  $a$  is a positive scalar,  $\beta_t$  is a random variable defined on  $Y$ , and  $\circ$  stands for the Schur (component-wise) product. Moreover we assume that  $\beta_t$  is an independent random variable with zero mean and variance  $R$  where  $R$  here is a vector containing the variance of each component and should not be confused with the covariance matrix. It can be seen that  $aM(x_t)^\theta \circ \beta_t$  represents the observation noise, controlled by two adjustable parameters  $\theta$  and  $a$ . It can be verified that the likelihood  $g_t(y_t|x_t)$  is of mean  $M(x_t)$  and variance  $a^2 M(x_t)^{2\theta} \circ R$ .

The parameter  $\theta$  is particularly important for specifying the noise model [11] and here we consider the following three representative cases. First if we take  $\theta = 0$ , it follows that  $y_t = M(x_t) + a\beta_t$ , where the observation noise is independent of the state value  $x_t$ . We refer to this case as the absolute noise. Second if  $\theta = 0.5$ , the variance of observation noise is  $a^2 M(x_t) \circ R$ , which is linearly dependent on  $M(x_t)$ , and we refer to this as the Poisson noise. Finally for  $\theta = 1$ , the standard deviation of the noise, equal to  $aM(x_t)R^{1/2}$ , depends linearly on  $M(x_t)$ , and this case is referred to as the relative noise. In our numerical experiments we test all the three cases. Moreover, in both of the two numerical examples provided in this work, we take  $M(x_t) = 0.1x_t^2$ ,  $a = 1$ , and  $\beta_t$  to follow the Student's t-distribution [12] with zero-mean and variance being 1.5.

### B. Lorenz-96 system

Our first example is the popular Lorenz-96 model [13]:

$$\begin{cases} \frac{dx^n}{dt} = (x^{n+1} - x_{n-2})x^{n-1} - x^n + 8, & n = 1, \dots, 40 \\ x^0 = x^{40}, & x^{-1} = x^{39}, & x^{41} = x^1, \end{cases} \quad (19)$$

and by integrating the system with the Runge-Kutta scheme with stepsize  $\Delta t = 0.05$ , and adding some model noise, we obtain the following discrete-time model:

$$\begin{cases} \mathbf{x}_t = \mathcal{F}(\mathbf{x}_{t-1}) + \alpha_t, & t = 1, 2, \dots \\ \mathbf{y}_t = M(\mathbf{x}_t) + M(\mathbf{x}_t)^\theta \beta_t, & t = 1, 2, \dots \end{cases} \quad (20)$$

where  $\mathcal{F}$  is the standard fourth-order Runge-Kutta solution of Eq. (19),  $\alpha_t$  is standard Gaussian noise, and the initial state  $\mathbf{x}_0 \sim U[1, 10]$ . We use synthetic data in this example, which means that both the true states and the observed data are simulated from the model.

As mentioned earlier, we consider the three cases  $\theta = 0, 0.5$  and  $1$ . In each case, we use two sample sizes  $M = 100$  and  $M = 20$ . To evaluate the performance of the LMEKF method, we implement it along with several commonly used methods: the extended EKF mentioned in Section III-B, PF, and NLEAF [2] with first-order (denoted as NLEAF 1) and second-order (denoted as NLEAF 2) correction, in the numerical tests. The stopping criterion in LMEKF is specified by  $\Delta_k = 20$  and  $\Delta_F = 0.1$ , while the step size  $\epsilon_k$  in GD iteration is  $0.001$ . For the small sample size  $M = 20$ , in all the methods except PF, the sliding window localization (with  $l = 3$  and  $k = 2$ ; see [2] for details) is used. With each method, we compute the estimator bias (i.e., the difference between the ensemble mean and the ground truth) at each time step and then average the bias over the 40 different dimensions. The procedure is repeated 200 times for each method and all the results are averaged over the 200 trials. The average bias for  $\theta = 0$  is shown in Fig. 1 where one can see that in this case, while the other three methods yield largely comparable accuracy in terms of estimation bias, the bias of LMEKF is significantly smaller. To analyze the convergence property of the method, in Figs. 2 (left) we show the number of GD iterations at each time step, where one can see that all GD iterations terminate after around 300-400 steps, except the iteration at  $t = 1$  which takes more than 700 steps. This can be further understood by observing Fig 2 (right) which shows the current best value  $F_k^*$  with respect to the GD iteration, where each curve represents the result at a time step  $t$ . One can see that the current best values become settled after around 400 iterations at all time locations except  $t = 1$ , which agrees well with the number of iterations shown on the left. These two figures thus show that the proposed stopping criteria are effective in this example. The same sets of figures are also produced for  $\theta = 0.5$  (Fig. 3 for the average bias and Fig. 4 for the number of iterations and the current best values) and for  $\theta = 1$  (Fig. 5 for the average bias and Fig. 6 for the number of iterations and the current best values). Conclusions drawn from these figures are largely the same as those for  $\theta = 0$ , where the key information is that LMEKF significantly outperforms the other methods in terms of estimation bias. Regarding the number of GD iterations in LMEKF, one can see that in these two cases (especially in  $\theta = 1$ ) it takes evidently more GD iterations for the algorithm to converge, which we believe is due to the fact that the noise in these two cases are not additive and so the observation models deviate further away from the Gaussian-linear setting. As has been mentioned we also conduct the experiments for a smaller sample size  $M = 20$  with localization employed, and we show the bias results for  $\theta = 0, \theta = 0.5$  and  $\theta = 1$  in Fig. 7. In this small sample size case, one can see that the advantage of LMEKF is not as large as that for  $M = 100$ , but nevertheless LMEKF still yields clearly the lowest bias among all the tested methods.

### C. Fisher equation model

Our second example is the Fisher's equation, a baseline model of wildfire spreading, where filtering is often needed to assimilate observed data at selected locations into the model [14]. Specifically, the

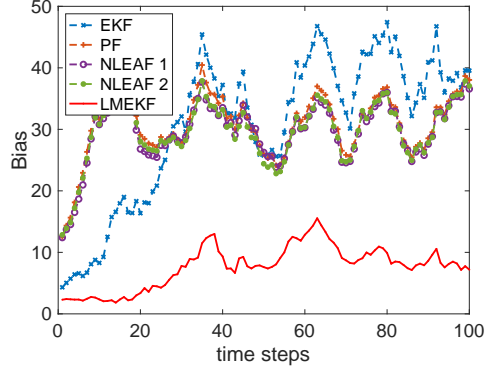


Fig. 1. The average bias at each time step for  $\theta = 0$  and  $M = 100$ .

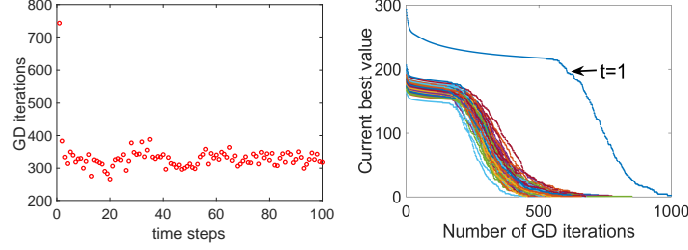


Fig. 2. Left: the number of GD iterations at each time step. Right: the current best value plotted against the GD iterations where each line represents a time step. The results are for  $\theta = 0$  and  $M = 100$ .

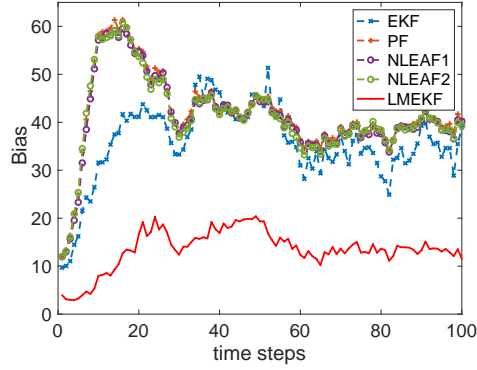


Fig. 3. The average bias at each time step for  $\theta = 0.5$  and  $M = 100$ .

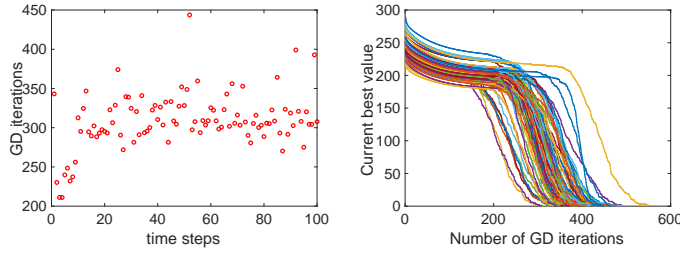


Fig. 4. Left: the number of GD iterations at each time step. Right: the current best value plotted against the GD iterations where each line represents a time step. The results are for  $\theta = 0.5$  and  $M = 100$ .

Fisher's equation is specified as follows,

$$c_t = Dc_{xx} + rc(1 - c), \quad 0 < x < L, \quad t > 0, \quad (21a)$$

$$c_x(0, t) = 0, \quad c_x(L, t) = 0, \quad c(x, 0) = f(x), \quad (21b)$$



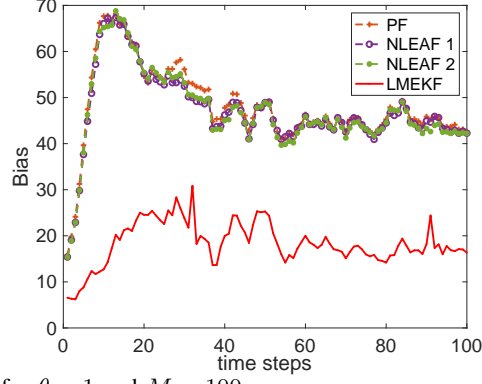


Fig. 5. The average bias at each time step for  $\theta = 1$  and  $M = 100$ .

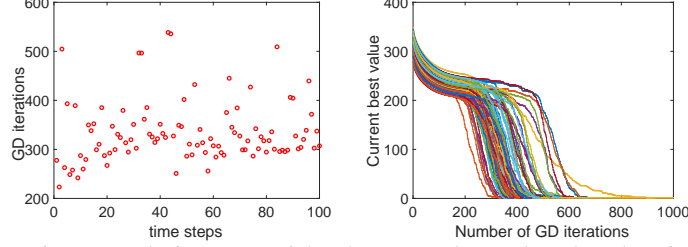


Fig. 6. Left: the number of GD iterations at each time step. Right: the current best value plotted against the GD iterations where each line represents a time step. The results are for  $\theta = 1$  and  $M = 100$ .

where  $D = 0.001$ ,  $r = 0.1$ ,  $L = 2$  are prescribed constants, and the noise-free initial condition  $f(x)$  takes the form of,

$$f(x) = \begin{cases} 0, & 0 \leq x < L/4 \\ 4x/L - 1, & L/4 \leq x < L/2 \\ 3 - 4x/L, & L/2 \leq x < 3L/4 \\ 0, & 3L/4 \leq x \leq L. \end{cases} \quad (22)$$

In the numerical experiments we use an upwind finite difference scheme and discretize the equation onto  $N_x = 200$  spatial grid points over the domain  $[0, L]$ , yielding a 200 dimensional filtering problem. The time stepsize is determined by  $D \frac{\Delta t}{\Delta x^2} = 0.1$  with  $\Delta x = \frac{L}{N_x - 1}$  and the total number of time steps is 60. The prior distribution for each grid point is  $U[-5, 5] + f(x)$ , and in the numerical scheme a model noise is added in each time step and it is assumed to be in the form of  $\mathcal{N}(0, C)$ , where  $C(i, j) = 0.3 \exp(-(x_i - x_j)^2 / L)$ ,  $i, j = 1, \dots, N_x$ , with  $x_i, x_j$  being the spatial positions. The observation model is as described in Section IV-A. We test the same set of filtering methods as those in the first example and 50 particles are used in each method. Since the sample size is smaller than the dimensionality, the sliding window localization with  $l = 5$  and  $k = 3$  is used. All the simulations are repeated 200 times and the average biases are plotted in Fig. 8 for all the three cases ( $\theta = 0, 0.5$  and 1). Once again, we see that in all the three cases the LMEKF method results in the lowest estimation bias among all the methods tested. It should be mentioned that, in the case that  $\theta = 1$ , the bias of EKF is enormously higher than those of the other methods and so is omitted in the figure. Since the bias results shown in Fig. 8 is averaged over all the dimensions, it is therefore also useful to examine the bias at each dimension. We therefore plot the bias at each grid point for the last time step in Fig. 9, where one can see that LMEKF yields substantially lower bias at the majority of the spatial points. We have also examined other time steps where the results are similar and therefore not presented here. We also report that, the wall-clock time for solving the optimization problem in each time step in LMEKF is approximately 2.0 seconds (on a personal computer with a 3.6GHz processor and 16GB RAM), indicating a modest computational cost in this 200 dimensional example.

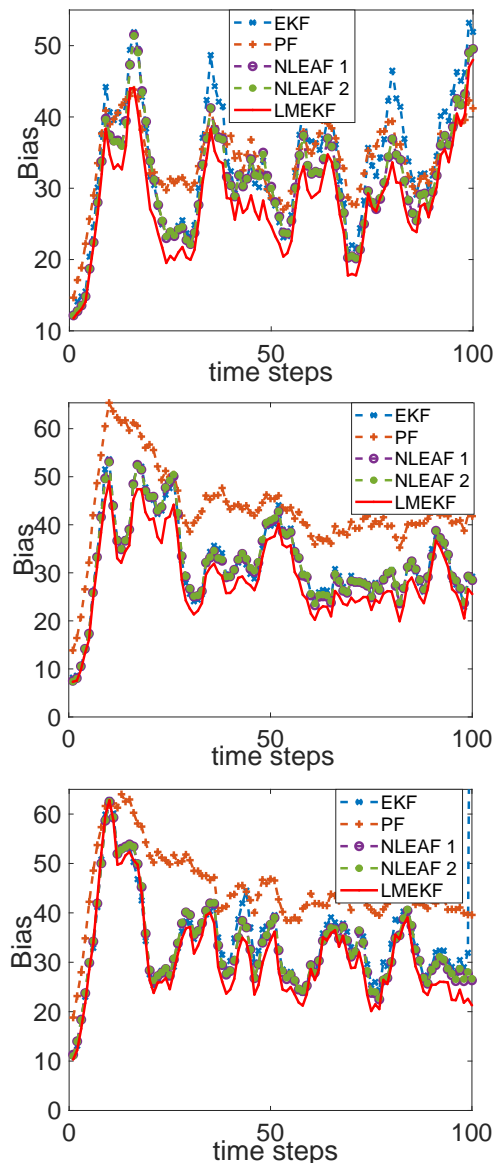


Fig. 7. The average bias at each time step for  $M = 20$ . From top to bottom are respectively the results  $\theta = 0, 0.5$  and  $1$ .

## V. CLOSING REMARKS

We conclude the paper with the following two remarks. First we emphasize that, though LMEKF can deal with generic observation models, it still requires that the posterior distributions are reasonably close to Gaussian, a requirement needed for all EKF type of methods; for strongly non-Gaussian posteriors, one may have to resort to other types of methods such as PF. Second we restate that, as is indicated in the Fisher’s equation example, the KLD minimization problem in LMEKF can be solved rather efficiently, and thus the updating step may not be the main contributor to the total computational burden, especially when the underlying dynamical model is computational intensive.

## REFERENCES

- [1] G. Evensen, *Data assimilation: the ensemble Kalman filter*. Springer Science & Business Media, 2009.
- [2] J. Lei and P. Bickel, “A moment matching ensemble filter for nonlinear non-gaussian data assimilation,” *Monthly Weather Review*, vol. 139, no. 12, pp. 3964–3973, 2011.
- [3] J. L. Anderson, “A local least squares framework for ensemble filtering,” *Monthly Weather Review*, vol. 131, no. 4, pp. 634–642, 2003.
- [4] —, “An ensemble adjustment kalman filter for data assimilation,” *Monthly weather review*, vol. 129, no. 12, pp. 2884–2903, 2001.

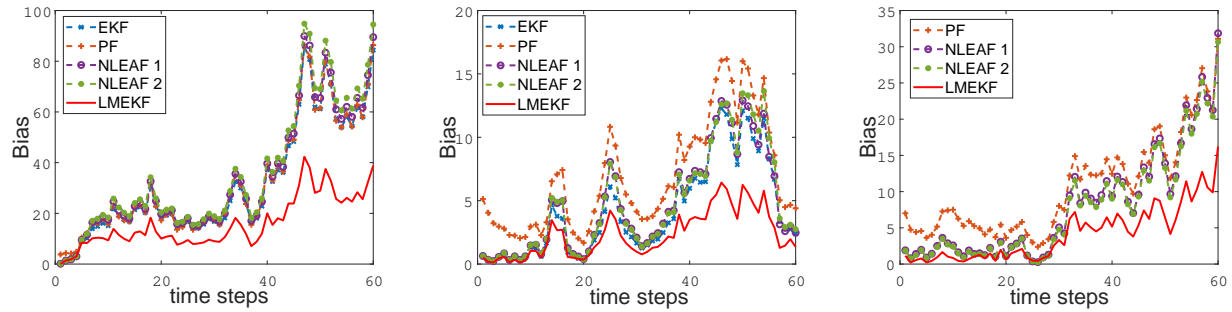


Fig. 8. The average bias at each time step. From left to right:  $\theta = 0$ ,  $\theta = 0.5$  and  $\theta = 1$ .

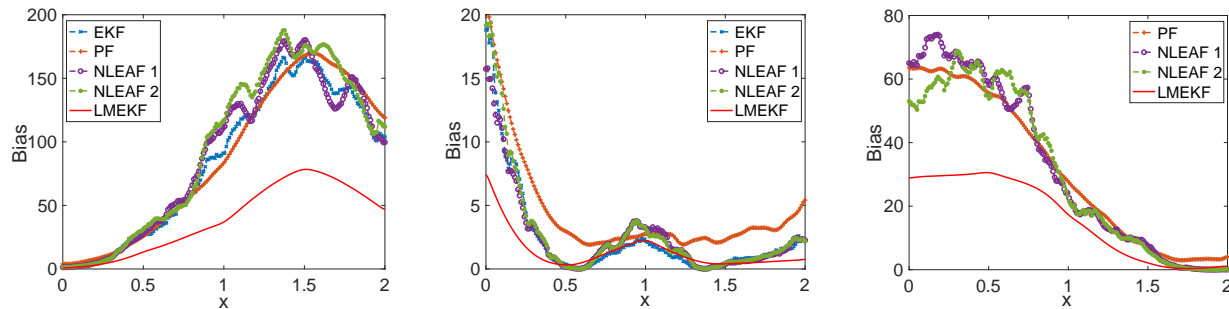


Fig. 9. The average bias at the final time step. From left to right:  $\theta = 0$ ,  $\theta = 0.5$  and  $\theta = 1$ .

- [5] P. L. Houtekamer and H. L. Mitchell, "A sequential ensemble kalman filter for atmospheric data assimilation," *Monthly Weather Review*, vol. 129, no. 1, pp. 123–137, 2001.
- [6] M. S. Arulampalam, S. Maskell, N. J. Gordon, and T. Clapp, "A tutorial on particle filters for online nonlinear/non-gaussian bayesian tracking," *IEEE Transactions on Signal Processing*, vol. 50, no. 2, pp. 174–188, 2002.
- [7] H. Auvinen, J. M. Bardsley, H. Haario, and T. Kauranne, "The variational kalman filter and an efficient implementation using limited memory bfgs," *International Journal for Numerical Methods in Fluids*, vol. 64, no. 3, pp. 314–335, 2010.
- [8] Z. Chen *et al.*, "Bayesian filtering: From kalman filters to particle filters, and beyond," *Statistics*, vol. 182, no. 1, pp. 1–69, 2003.
- [9] T. A. El Moselhy and Y. M. Marzouk, "Bayesian inference with optimal maps," *Journal of Computational Physics*, vol. 231, no. 23, pp. 7815–7850, 2012.
- [10] E. Ott, B. R. Hunt, I. Szunyogh, A. V. Zimin, E. J. Kostelich, M. Corazza, E. Kalnay, D. Patil, and J. A. Yorke, "A local ensemble kalman filter for atmospheric data assimilation," *Tellus A: Dynamic Meteorology and Oceanography*, vol. 56, no. 5, pp. 415–428, 2004.
- [11] A. Capaldi, S. Behrend, B. Berman, J. Smith, J. Wright, and A. L. Lloyd, "Parameter estimation and uncertainty quantification for an epidemic model," *Mathematical biosciences and engineering*, p. 553, 2012.
- [12] M. Roth, E. Özkan, and F. Gustafsson, "A student's t filter for heavy tailed process and measurement noise," in *2013 IEEE International Conference on Acoustics, Speech and Signal Processing*, 2013, pp. 5770–5774.
- [13] E. N. Lorenz, "Predictability: A problem partly solved," in *Proc. Seminar on predictability*, vol. 1, no. 1, 1996.
- [14] J. Mandel, L. S. Bennethum, J. D. Beezley, J. L. Coen, C. C. Douglas, M. Kim, and A. Vodacek, "A wildland fire model with data assimilation," *Mathematics and Computers in Simulation*, vol. 79, no. 3, pp. 584–606, 2008.